Drug Design, Development and Therapy

Dovepress
open access to scientific and medical research

Open Access Full Text Article

ORIGINAL RESEARCH

Pharmacological Activity of Matrine in Inhibiting Colon Cancer Cells VM Formation, Proliferation, and Invasion by Downregulating Claudin-9 Mediated EMT Process and MAPK Signaling Pathway

Qiu Du[1,2,*], Yingda Lin[3,4,*], Changping Ding[5,*], Ling Wu[3], Yuan Xu[3], Qingling Feng[6]

[1]Department of Neurosurgery, the Affiliated Hospital of Yangzhou University, Yangzhou University, Yangzhou, 225012, People's Republic of China; [2]Department of Central Laboratory, the Affiliated Hospital of Yangzhou University, Yangzhou University, Yangzhou, 225012, People's Republic of China; [3]Department of Pharmacy, the Affiliated Hospital of Yangzhou University, Yangzhou University, Yangzhou, 225012, People's Republic of China; [4]Department of Pharmacy, Dongzhimen Hospital, Beijing University of Chinese Medicine, Beijing, 100700, People's Republic of China; [5]Department of Medical Laboratory, the Affiliated Hospital of Yangzhou University, Yangzhou University, Yangzhou, 225012, People's Republic of China; [6]Department of Emergency Intensive Care Unit, the Affiliated Hospital of Yangzhou University, Yangzhou University, Yangzhou, 225012, People's Republic of China

*These authors contributed equally to this work

Correspondence: Qingling Feng, Department of Emergency Intensive Care Unit, the Affiliated Hospital of Yangzhou University, Yangzhou University, 368 Hanjiang Middle Road, Yangzhou, 225012, People's Republic of China, Email 15216401512@163.com; Yuan Xu, Department of Pharmacy, the Affiliated Hospital of Yangzhou University, Yangzhou University, 368 Hanjiang Middle Road, Yangzhou, 225012, People's Republic of China, Email feebyxuyuan@163.com

Purpose: Matrine (Mat), the main active ingredient of traditional Chinese herbal plant *Sophora flavescens Ait*, has significant antitumor effects, but its pharmacological mechanism on colon cancer (CC) remains unclear. This study aimed to investigate the therapeutic effect of Mat on CC as well as the potential mechanism.

Methods: The vasculogenic mimicry (VM) of CC cells was observed by three-dimensional (3D) Matrigel cell culture. Cell proliferation, apoptosis, migration, invasion, and actin filament integrity were detected by CCK8, flow cytometry, wound healing, Transwell and Phalloidin staining assays. qRT-PCR and Western blotting were applied to detect the expression of EMT factors. RNA-sequencing was conducted to screen differentially expressed genes (DEGs), and the GO and KEGG pathway enrichment analyses were performed. Then, the expression of the key MAPK pathway genes and the target gene Claudin-9 (Cldn9) were analyzed. RNA interference was used to silence Cldn9 expression, and the effects of Cldn9 silencing and simultaneous treatment with Mat on VM formation, proliferation, apoptosis, invasion, and migration were investigated. Finally, the expression of EMT factors and MAPK pathway key genes was detected.

Results: CT26 cells formed the most typical VM structure. Mat disrupted the VM of CT26 cells, significantly suppressed their proliferation, migration, invasion, actin filament integrity, induced apoptosis, and inhibited EMT process. RNA-sequencing revealed 163 upregulated genes and 333 downregulated genes in Mat-treated CT26 cells, and the DEGs were significantly enriched in cell adhesion molecules and MAPK signaling pathways. Further confirmed that Mat significantly inhibited the phosphorylation levels of JNK and ERK, and the target gene Cldn9 was significantly upregulated in human CC tissues. Silencing Cldn9 markedly inhibited the VM, proliferative activity, invasiveness, and actin filament integrity of CT26 cells, blocked the EMT process, and downregulated the phosphorylation of JNK and ERK, whereas Mat intervention further strengthened the above trends.

Conclusion: This study indicated that Mat may synergistically inhibit the EMT process and MAPK signaling pathway through downregulation Cldn9, thereby exerting pharmacological effects on inhibiting VM formation, proliferation, and invasion of CC cells.

Keywords: matrine, colon cancer, Cldn9, EMT, MAPK signal pathway

Introduction

According to the latest global cancer data released by the International Agency for Research on Cancer (IARC) in 2020, colorectal cancer (CRC) has become the third most common cancer worldwide, accounting for approximately 10% of

Received: 26 April 2023
Accepted: 25 August 2023
Published: 11 September 2023

new cancer cases. It is also the second most common cause of cancer mortality, accounting for approximately 9.4% of cancer deaths. As morbidity and mortality from CC have increased significantly, the health threat from this disease is becoming increasingly serious.[1] As a clinically common and highly malignant cancer of the digestive tract, CC is commonly treated with cytotoxic (5-fluorouracil, oxaliplatin, irinotecan, capecitabine) and biological chemotherapeutic drugs (bevacizumab, panitumumab, cetuximab).[2] These treatments can extend the survival of some patients with CC. However, due to the complex etiology of this malignant cancer, the current clinical use of anti-CC drugs results in unavoidable side effects. Approximately 30% of CC patients have metastatic disease accompanied by symptoms of bleeding or obstruction.[3,4] Therefore, the development of new, effective anti-CC drugs is urgently needed.

Traditional Chinese medicine (TCM), which is thousands of years old, is now widely accepted as an alternative treatment for cancer. Many cancer patients use TCM as a potential treatment due to its significant efficacy and lack of serious side effects.[5] Mat (molecular formula: C15H24N2O, molecular weight: 248.36 g/mol), the main active ingredient of the traditional Chinese herbal plant *Sophora flavescens Ait*, is widely present in the leguminous plants *Sophora alopecuroides Linn* and *Sophora tonkinensis*.[6] As a tetracyclic quinazine alkaloid with potent properties, Mat has been approved by the China Food and Drug Administration (CFDA) for the prevention and treatment of cancer cachexia.[7] Many studies have shown that Mat has excellent anti-tumor activity and shows inhibitory effects in various tumor types such as liver cancer, leukemia, multiple myeloma, and gastric cancer. It has also been shown to regulate multiple signaling pathways related to tumor proliferation, apoptosis, angiogenesis, invasion, and migration.[8,9]

Tumor angiogenesis is a basic biological process occurring during tumor growth and metastasis. Previous studies had stated that endothelium-dependent angiogenesis is the only mechanism for satisfying the increased tumor blood supply. However, a newly defined tumor microangiogenesis model called vasculogenic mimicry (VM) has attracted much attention. Studies have found that VM forms in a manner similar to embryonic angiogenesis. Highly invasive tumor cells that engage in VM simultaneously express markers of endothelial cells and tumor cells, generating functional blood vessels containing red blood cells to provide nutrition for rapidly growing tumors. This is closely related to tumor pathological grade, low survival rate, invasion, and metastasis.[10,11] Baeten et al[12] found that 23 (19.7%) of 117 CC patient tumor samples had VM with high expression of EPHA2 and LAMC2, and the existence of VM was associated with significantly shortened survival. Song et al[13] showed that a high-fat diet significantly promoted VM formation in CRC and changed the intestinal microflora composition of APC mice. Additionally, the microbial metabolite DCA significantly promoted VM formation and EMT through the activation of VEGFR2, thus further aggravating intestinal cancerization. In addition, Hou et al[14] found that Yi Ai Fang, a traditional Chinese herbal formula, restrained the formation of VM in CRC through the HIF-1α/EMT pathway and significantly inhibited tumor growth. Studies suggest that VM inhibition is a promising strategy for drug therapy in CC.[15,16] However, whether Mat inhibits tumor cell proliferation and invasion by impacting VM formation has not been reported.

Although Mat has been shown to have an antitumor effect on CC,[17–19] its underlying mechanism of action remains unclear. In the present study, we investigated the effects of Mat on VM formation, proliferation, migration, and invasion in CC cells, and analyzed significantly enriched DEGs in signaling pathways by transcriptome sequencing combined with bioinformatics. Results demonstrated that Mat may reverse the EMT process and mediate the MAPK signaling pathway through down-regulation Cldn9 to inhibit VM formation, proliferation, and invasion in CC cells. These results emphasized that Cldn9 may be a potential therapeutic target for CC.

Materials and Methods

Clinical Samples

A total of 17 human CC tissues and 5 normal colon tissues were obtained from patient surgical resections in the Department of Oncology at the Affiliated Hospital of Yangzhou University from July 2020 to June 2021. The baseline characteristics of these CC patients are shown in Table 1. Written informed consent was obtained from all patients whose tumor tissues were used in this study. The study was approved by the Ethics Committee of the Affiliated Hospital of Yangzhou University and complied with the Declaration of Helsinki.

Table 1 Clinical and Immunohistochemical Characteristics of 17 Colon Cancer Patients

No.	Gender	Age at Onset (Years)	Tumor Size (mm)	Differentiation Degree	MLH1	MSH2	MSH6	PMS2	Her2	Villin	CK7	CK20	Ki-67	CDH17
1	F	60	55×55×8	Medium-low	–	+	+	–	NT	+	NT	–	80%, +	+
2	M	80	60×45×45	Medium-low	+	+	+	+	1+	NT	NT	NT	70%, +	NT
3	M	43	20×20×6	Medium	–	+	+	–	2+	NT	NT	NT	80%, +	NT
4	M	73	10×8×5	Medium-low	+	+	+	+	1+	+	–	+	80%, +	NT
5	M	37	50×40×8	Medium	–	+	+	–	NT	NT	NT	NT	60%,+	NT
6	F	84	60×45×10	Medium	+	+	+	+	1+	NT	NT	NT	4%,+	NT
7	F	54	30×25×10	Medium	+	+	+	+	+	NT	NT	NT	60%,+	+
8	F	67	45×40×20	Low	–	–	+	–	+	+	NT	–	HS, 60%,+	NT
9	M	64	55×55×20	Medium-low	+	+	+	+	0	+	–	–	80%,+	NT
10	F	72	30×30×8	Medium	+	+	+	+	2+	+	–	+	30%,+	NT
11	M	73	50×30×10	Medium	+	+	+	+	NT	NT	NT	NT	70%,+	NT
12	M	68	55×35×8	Medium	+	+	+	+	+	NT	NT	NT	15%,+	+
13	F	72	35×35×12	Medium	+	+	+	+	2+	NT	NT	NT	20%,+	+
14	F	69	30×30×8	Medium	+	+	+	+	1+	NT	NT	NT	30%,+	+
15	M	60	50×50×25	Medium	+	Partial,+	+	Partial,+	1+	+	–	+	30%,+	NT
16	F	63	60×50×40	Medium	+	+	+	+	1+	+	–	+	60%,+	NT
17	M	65	90×80×50	Medium-low	+	–	–	Few,+	0	Partial,+	+	Partial,+	70%,+	NT

Abbreviations: +, positive; –, negative; F, female; M, male; HS, hot spot; NT, Not test.

https://doi.org/10.2147/DDDT.S417077

Cell Culture

Human CC cell lines (HCT116, SW480, and KM12) and the mouse CC cell line CT26 were obtained from the Cell Resource Center, Peking Union Medical College (headquarters of the National Science & Technology Infrastructure, National BioMedical Cell-Line Resource, NSTI-BMCR). All cell lines were authenticated by Short Tandem Repeat (STR) assay. All cells were cultured in Dulbecco's Modified Eagle's Medium (DMEM) medium supplemented with 10% fetal bovine serum (FBS, Procell, Wuhan, China), 100 U/mL penicillin, and 100 mg/mL streptomycin (Invitrogen) and maintained at 37°C in a humidified incubator with 95% air and 5% CO_2. To evaluate the effects of Mat on cells, Mat (≥99% by HPLC, HY-N0164) was purchased from MedChemExpress Co., Ltd (Monmouth Junction, NJ, USA), dissolved in dimethyl sulfoxide (DMSO) (Sigma Aldrich, Merck KGaA, Germany) as a stock solution (100 mM), and further diluted to different concentrations with PBS.

3D Cell Culture

Matrigel was dissolved overnight at 4°C, 24-well plates were pre-cooled (Corning Life Sciences, NY, USA), and pipette tips were kept at 4°C. The 24-well plates were placed on ice and 200 μL cold Matrigel was added to each well. Plates were shaken gently to ensure the Matrigel evenly covered the bottom of each well and then placed at 37°C for 30 min to gel. Each CC cell line was used in the logarithmic growth stage. Cells were inoculated in DMEM at a cell density of 6×10^5 cells/well in a 24-well plate covered with Matrigel. Plates were then cultured in a 37°C cell incubator with saturated humidity and 5% CO_2. VM structure formation between cells was observed and photographed under an inverted microscope (Nikon, Tokyo, Japan) every 6 h; the culture was terminated after 24 h.

Cell Proliferation Assay

The Cell Counting Kit-8 (CCK-8, Dojindo Laboratories, Japan) was used to analyze cell proliferation according to the manufacturer's instructions. In brief, 5×10^3 cells resuspended in 100 μL of complete medium were seeded in each well of 96-well plates. After 8 h, Mat was added at a final concentration of 0, 0.25, 0.5, or 1 mM. After 24-or 48-h treatment, 10 μL CCK8 solution was added to each well. After incubation for 2 h, the absorbance at 450 nm was detected using a Microplate Reader (Thermo Fisher Scientific, Waltham, MA, USA).

Flow Cytometric Apoptosis Assay

The cells were seeded in 12-well plates at an appropriate density and then treated with Mat at different concentrations or transfected when the confluence reached approximately 60–80%. After 24 h or 48 h, the cells in each group were digested with trypsin without EDTA and collected by centrifugation. Then, the FITC Annexin V Apoptosis Detection Kit I (BD Biosciences, Franklin Lakes, NJ, USA) was used for apoptosis detection according to the manufacturer's instructions. Cells were analyzed using CytExpert Software under a FACS flow cytometer (Beckman Coulter, Inc., Brea, CA, USA).

Cell Scratch Assay

Cells were resuspended, inoculated in 6-well plates with 7.5×10^5 cells per well, and incubated until the confluence reached more than 90%. Horizontal scratches were made with a 200-μL pipette tip perpendicular to the 6-well plate. Then, each well was washed with PBS three times, and the serum-free medium containing Mat at a final concentration of 0, 0.25, 0.5, or 1 mM was added to each well. The culture was continued in the incubator and wound healing was observed at 0, 24, and 48 h after scratching under an inverted microscope (Nikon). The ImageJ software was used to quantify cell migration by measuring the distance between the two edges of the wound.

Cell Migration and Invasion Assay

As described in our previous study,[20] the cell migration and invasion assays were performed with Transwell Chamber 24-Well Plates and Corning Matrigel Invasion Chambers with 8-μm pore size membranes (Corning), respectively.

Phalloidin Staining Assay

Cells were seeded and grown on glass coverslips in 6-well plates at an appropriate density. Following cell adhesion, Mat was added at final concentrations of 0.25, 0.5, and 1 mM and the culture continued for 24 or 48 h. After discarding the medium, cells were fixed with 4% paraformaldehyde for 15 min and then washed with PBS three times. Cells were then incubated with 0.1% Triton X-100 for 5 min to increase permeability. Finally, the cells were stained with 200 nM FITC-Phalloidin, sealed with DAPI Fluoromount-G™, and observed under a confocal laser scanning microscope (A1, Nikon, Tokyo, Japan).

RNA Sequencing Analysis

Mat-treated CT26 cells and control cell samples were sent to Novogene (Novogene Co., Ltd., Bejing, China) for quality control and RNA integrity analysis followed by library preparation, and sequencing, and the data were analyzed on the free online platform of Novogene Cloud Platform (www.novogene.com). Differentially expressed genes (DEGs) were analyzed using the DESeq2 R package. DEGs were screened using padj ≤ 0.05. The ClusterProfiler software package was used to conduct gene ontology (GO) enrichment analysis of differentially expressed genes. GO terms with padj ≤ 0.05 were considered significantly enriched.

qRT-PCR Analysis

Total RNA was extracted from cells using TRIzol reagent (Thermo Fisher Scientific), and RNA concentration was detected using an ultramicro spectrophotometer (Thermo Fisher Scientific). RNA was then reverse transcribed into cDNA using PrimeScript RT Master Mix (Takara, Dalian, China). qRT-PCR amplification was conducted using Hieff® qPCR SYBR Green Master Mix (Yeasen, Shanghai, China) according to the manufacturer's instructions in a CFX96 Touch Real-Time PCR Detection System (Bio-Rad Laboratories, Inc., Hercules, CA, USA). Data quantification was normalized to GAPDH mRNA expression levels using the $2^{-\Delta\Delta Ct}$ method. The primers used were synthesized by Sangon Biotech Co., Ltd. (Shanghai, China); the sequences are shown in Table 2.

Cell Transfection

The small interfering RNA (siRNA) specific to Cldn9 and the negative control were designed and synthesized by GENEWIZ Biotechnology Co., Ltd. (Suzhou, China). siRNA was transfected into cells using Lipofectamine 3000 (Invitrogen, Carlsbad, CA, USA) according to the manufacturer's protocol. After 48 h of transfection, the knockdown efficiency of Cldn9 was detected by the qRT-PCR assay. The sequences of the Cldn9 siRNA are shown in Table 3.

Table 2 Sequences of the Primers Used in the qRT-PCR

Gene	Primer (5'-3')	Reverse Primer (5'-3')
E-cadherin (mouse)	AACCCAAGCACGTATCAGGG	ACTGCTGGTCAGGATCGTTG
N-cadherin (mouse)	AGTGGCAGGTAGCTGTAAAC	TGGCAAGTTGTCTAGGGAATAC
MMP2 (mouse)	GCTGTATTCCCGACCGTTG	TGGTCCGCGTAAAGTATGGG
MMP9 (mouse)	ACGACATAGACGGCATCCAGTATC	AGGTATAGTGGCACACATAGTGGG
GAPDH (mouse)	AACAGCAACTCCCACTCTTC	CCTGTTGCTGTAGCCGTATT
Aldh3a1 (mouse)	CACTTCCAGCGGGTCATAAA	TAGGATGGTGGGAGCTATGT
Gstp2 (mouse)	TCTGGACTCTTTCCCGTCTCTCAA	ATTCACTGTTTGCCGTTGCCGT
Jam3 (mouse)	GGGAGTCCTTGTTGTCCTTATT	CCTGGGCTCTTATAGCTTTCTC
Claudin9 (mouse)	GAACGCGGTTGTTCCTAGTT	TAGGTCCCGCTCATCTGTATT
Claudin18 (mouse)	TCCACGGCCTTAGTACTCATA	CCAGACACACAGGTCTCTATTG
Hspa2 (mouse)	AAATGCGGTGGAGTCCTATAC	TGTCCTGCTCGCTAATCTTG
Efna4 (mouse)	GGGCTTCAACGATTACCTAGA	CTGACCAGTCCACCATGTATAA
Efna1 (mouse)	GAAGAGACTCCAAGCAGATGAC	CAGCAGTGGTAGGAGCAATAC
Mapkapk5 (mouse)	GAAGGTCAAACCAGAGGAAAGA	GGCAGAGGGTAGCACATTATC
E-cadherin (human)	CGACCCAACCCAAGAATCTATC	AGGTGGTCACTTGGTCTTTATTC
N-cadherin (human)	GGATGAAACGCCGGGATAAA	TCTTCTTCTCCTCCACCTTCTT
MMP2 (human)	AAGTGGTCCGTGTGAAGTATG	GGTATCAGTGCAGCTGTTGTA
MMP9 (human)	GAACTTTGACGACAAGAAG	CGGCACTGAGGAATGATCTAA
GAPDH (human)	GGAGCGAGATCCCTCCAAAAT	GGCTGTTGTCATACTTCTCATGG

Table 3 Cldn9 siRNA Sequences

Gene	Primer (5'-3')	Reverse Primer (5'-3')
si-NC	UUCUCCGAACGUGUCACGUTT	ACGUGACACGUUCGGAGAATT
si-Cldn9-1	GCAAAGUAUACGACUCACUTT	AGUGAGUCGUAUACUUUGCTT
si-Cldn9-2	GCCUUGAACUCCUCGGCAUTT	AUGCCGAGGAGUUCAAGGCTT

Immunohistochemical Analysis

Immunohistochemistry was performed according to a previous method.[21] Briefly, the tissue sections were dipped in xylene and a series of ethanol gradients to dewax and rehydrate them. After antigen retrieval and endogenous peroxidase activity were blocked, the sections were incubated with target antibodies overnight at 4°C. After washing with PBS three times, the sections were incubated with biotinylated secondary antibody followed by addition of streptavidin-HRP, DAB staining, and hematoxylin counterstaining. Finally, pictures were captured with an inverted microscope (Nikon) and analyzed using ImageJ software (Media Cybernetics, Inc., Rockville, MD, USA).

Western Blot Analysis

The Western blot assay was performed as previously described.[22] Signal detection was performed using the ultrasensitive ECL plus Detection Reagent (Millipore Corporation, Billerica, MA, USA) on the Invitrogen iBright™ CL1500 Imaging System (Thermo Fisher Scientific), and analyzed using ImageJ software.

Statistical Analysis

All experiments were repeated at least three independent times and the data are expressed as mean ± standard deviation (SD). Significance analysis was performed using GraphPad Prism 9.0 (GraphPad Software, San Diego, CA, USA). Significant differences were determined by Student's *t*-test or one-way analysis of variance (ANOVA). A $p < 0.05$ was considered statistically significant.

Results

Mat Inhibited VM Formation and Cell Proliferation in CC Cells

SW480, HCT116, and KM12 human CC cell lines and mouse CC cell line CT26 were selected for 3D culture in Matrigel, and the difference of VM formation in each cell was compared 24 hours later. The results showed that CT26 cells formed the most typical VM structure, SW480 cells formed irregular VM, while other cells did not form clear VM (Figure 1A). Therefore, we selected CT26 cells for subsequent experiments. Next, CT26 cells were treated with different concentrations of Mat (0mM, 0.25mM, 0.5mM, 1mM, 2mM, 3mM, and 4mM) and found that Mat significantly inhibited the proliferation of CT26 cells in a time and concentration dependent manner (Figure 1B), with IC50 values of 1.397 mM and 0.9088 mM for 24 and 48 h (Figure 1C), respectively. We then treated CT26 cells with 0mM, 0.25mM, 0.5mM, and 1mM Mat, and the effects of different treatment times (6h, 12h, and 24h) on VM formation were detected. The results showed that Mat treatment destroyed the VM lumen structure of CC CT26 cells, resulting in a significant reduction in VM number in a time- and concentration-dependent manner (Figure 1D).

Mat Promoted CT26 Apoptosis and Inhibited Cell Migration, Invasion, and Actin Filament Integrity

Next, we analyzed the effect of Mat on the apoptosis of CT26 cells by flow cytometry. Results showed that compared with the control group, Mat treatment significantly increased the percentage of apoptotic cells in a time-dependent and dose-dependent manner (Figure 2A), suggesting that Mat significantly promoted apoptosis in CC cells. Then, the effects of Mat on the migration and invasion of CT26 cells were detected by scratch healing and transwell assays. We found that Mat inhibited cell mobility and invasiveness gradually and more significantly with increasing concentration and time compared to the control group (Figure 2B–D). Phalloidin tightly and selectively binds to filamentous actin (F-actin) to

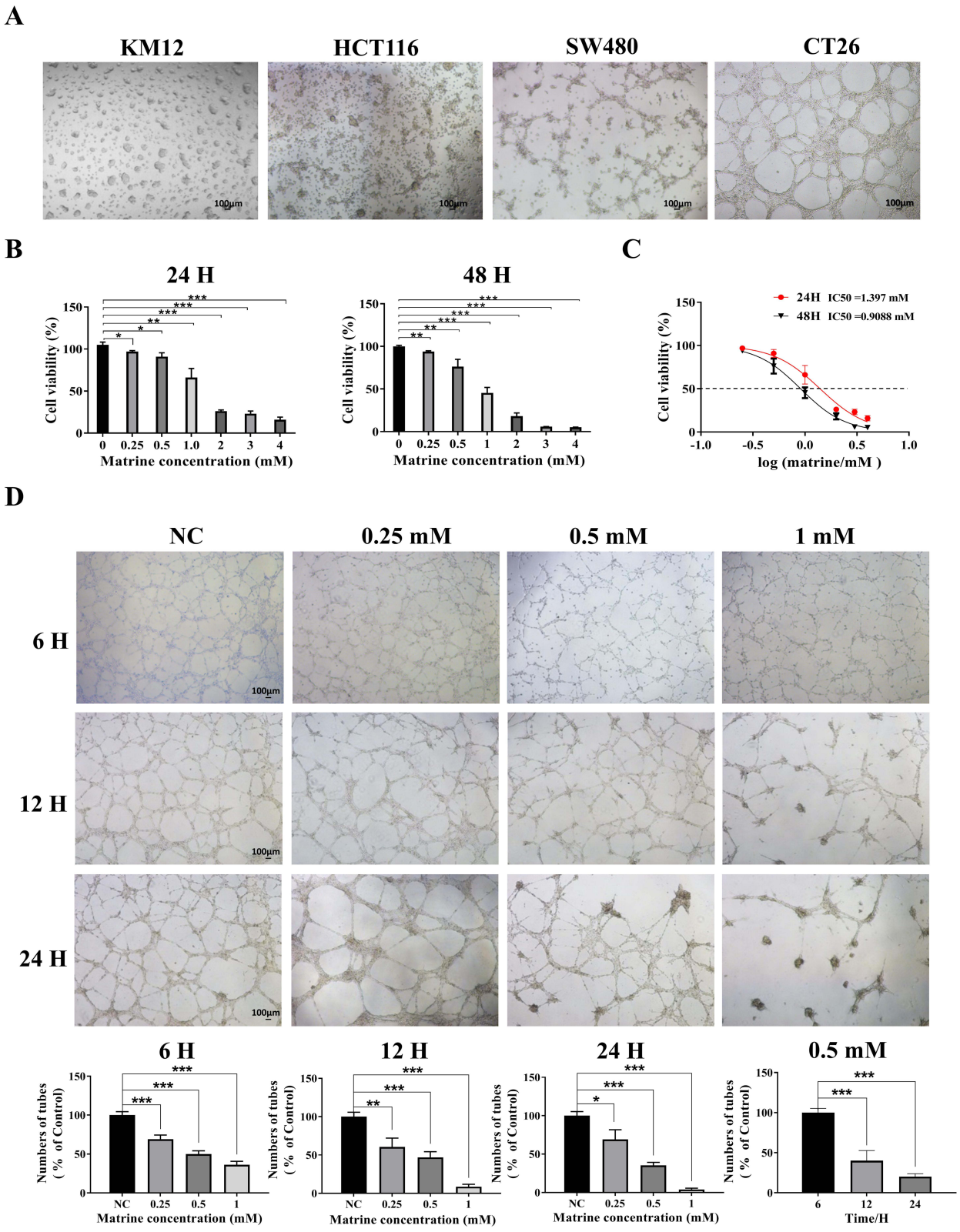

Figure 1 VM formation of different CC cell lines and the effects of Mat on cell proliferation and VM formation.

Notes: (**A**) The difference in VM formation of SW480, HCT116, KM12, and CT26 cells on Matrigel. Scale bars represent 100 μm; (**B**) The effect of Mat on the viability of CT26 cells; (**C**) IC50 values of Mat on CT26 cells at 24 and 48 h; (**D**) The effect of Mat on VM formation in CT26 cells. Scale bars represent 100 μm. *p<0.05; **p<0.01; ***p<0.001.

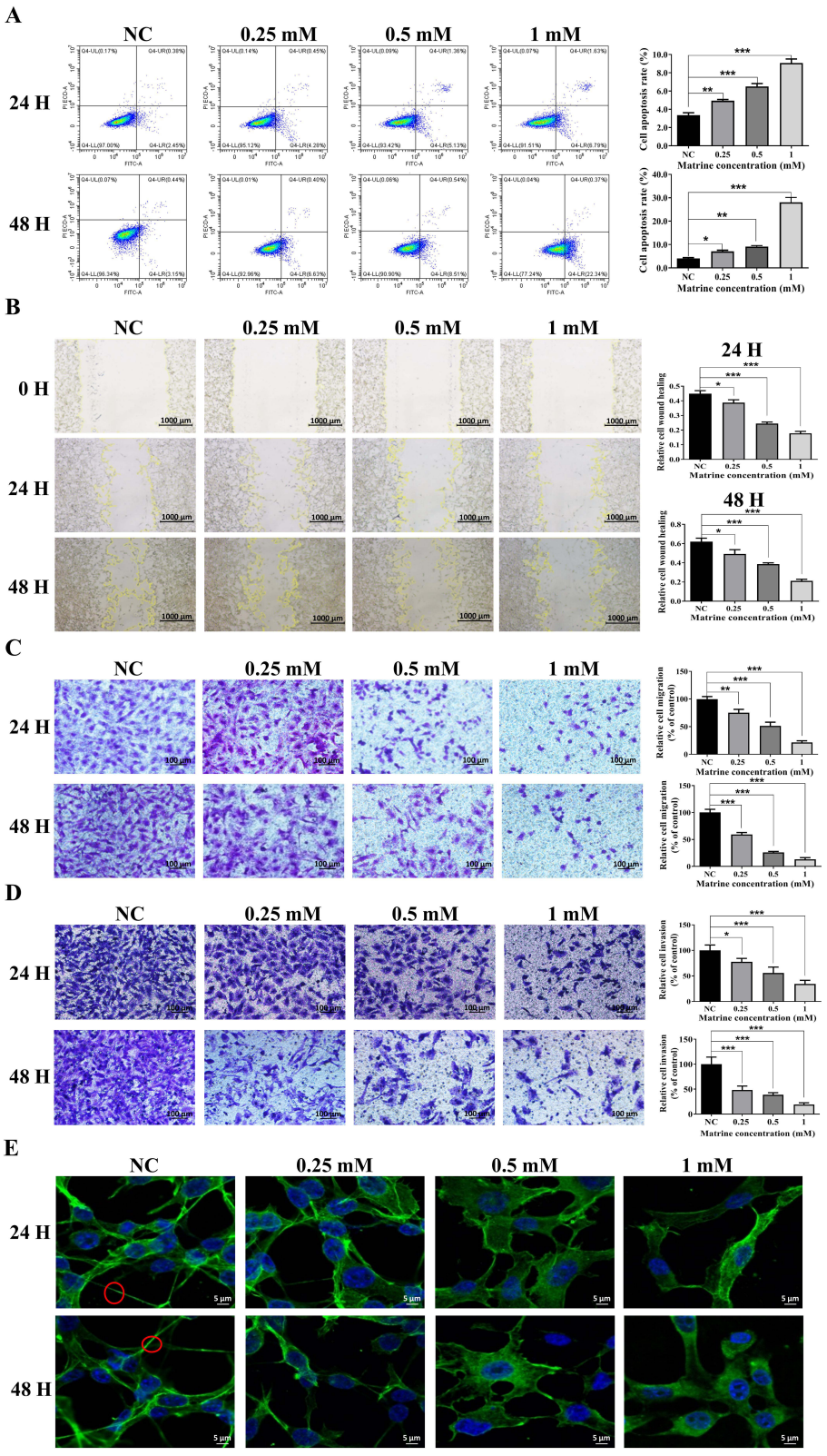

Figure 2 The effects of Mat on CT26 cells apoptosis, migration, invasion, and actin filament integrity.

Notes: (**A**) The apoptosis of CT26 cells treated with Mat; (**B**) The effect of Mat on CT26 cells migration by scratch healing assay. Scale bars represent 1000 μm; (**C**) The effect of Mat on CT26 cells migration by Transwell assay. Scale bars represent 100 μm; (**D**) The effect of Mat on CT26 cells invasion by Transwell assay. Scale bars represent 100 μm; (**E**) The effect of Mat on actin filament integrity in CT26 cells by phalloidin staining. The red circles indicate typical actin filaments. Scale bars represent 5 μm. *p<0.05; **p<0.01; ***p<0.001.

reveal the distribution of the microfilament skeleton in cells. Therefore, phalloidin staining was used to investigate the effect of Mat upon changes in actin filament integrity in CC cells. The results showed that with the increase of Mat dose and treatment duration, the microfilament morphology between CT26 cells was destroyed and the aggregation degree was gradually reduced (Figure 2E), indicating that Mat altered the integrity of actin filaments in CC cells. Due to the fact that actin filaments are a part of the cytoskeleton and play a crucial role in many cellular functions such as cell stability, adhesion, and motility, it is suggested that Mat may regulate the invasion and migration of CC cells by disrupting the integrity of actin filaments.

Mat Inhibited VM Formation in CT26 Cells Through Epithelial-Mesenchymal Transition (EMT)

Studies have shown that EMT plays an important role in the formation mechanism of VM.[23,24] To further verify this, qRT-PCR and Western blotting were used to determine the effects of Mat on the key EMT factors E-cadherin, N-cadherin, MMP2, and MMP9. The results showed that compared with the control group, Mat treatment significantly downregulated the mRNA and protein expression levels of N-cadherin, MMP2, and MMP9 while upregulating the E-cadherin levels (Figure 3A and B). Further, we observed that the mRNA expression of N-cadherin, MMP2, and MMP9 in SW480 human CC cells was significantly downregulated after Mat treatment, where E-cadherin expression was upregulated (Figure 3C). These results were consistent with the trends seen in CT26 cells and suggest that Mat may inhibit VM formation through an EMT-dependent mechanism.

Analysis of Differentially Expressed Genes (DEGs) in Mat-Treated CT26 Cells

To further clarify the signaling pathways and target genes that Mat may modulate, the DEGs of CT26 cells treated with Mat were analyzed by transcriptome sequencing. The results showed that 163 genes were significantly upregulated and 333 genes were significantly downregulated (| log2 Fold Change |>1, and $p < 0.05$) (Figure 4A). These DEGs were further analyzed through Gene Ontology (GO) and Kyoto Encyclopedia of Genes and Genomes (KEGG) pathway analysis to clarify their significant correlations with different cellular biological functions or signaling pathways. GO analysis showed that the DEGs were remarkably enriched in fluid transport, extracellular matrix, receptor regulator activity of cellular component (CC), biological process (BP), and molecular function (MF) (Figure 4B). KEGG pathway analysis showed that the DEGs were significantly enriched in the metabolism of xenobiotics by cytochrome P450, cell adhesion molecules, and MAPK signaling pathways (Figure 4C). Next, qRT-PCR was used to verify the expression of partial DEGs enriched in these three signaling pathways. The results showed that mRNA expression of the Aldh3a1 and Gstp2 genes enriched in the metabolism of xenobiotics by the cytochrome P450 pathway, Jam3, Cldn9, and Claudin-18 genes (which are enriched in the cell adhesion molecules pathway), and Efna4, Efna1, Mapkapk5, Angpt2, and Hspa2 genes (which are enriched in the MAPK signaling pathway) were significantly downregulated (Figure 4D–F). These results were consistent with the sequencing results. Further, we tested whether Mat plays a pharmacological role through the MAPK signaling pathway. Results showed that Mat treatment significantly inhibited the phosphorylation levels of JNK and ERK in CT26 cells compared with the control group (Figure 4G), indicating that Mat may inhibit the growth of CC cells through the MAPK signaling pathway.

It has been reported that cell adhesion molecules mediate the contact and conjunction between cells or between cells and the extracellular matrix to promote signal transduction, cell growth, wound healing, and vascular growth. This also plays a key role in tumor invasion, recurrence, and distant metastasis.[25] It was observed that Cldn9, which is significantly enriched in this pathway, had the highest expression and was obviously downregulated among the verified DEGs. Therefore, Cldn9 attracted our interest. Further, we confirmed that the expression of Cldn9 in CC tissues was significantly upregulated compared with normal colon tissues (Figure 5A–C). These results suggested that Mat may inhibit CC VM formation, cell proliferation, invasion, and migration through the MAPK signaling pathway. However, whether Mat serves a pharmacological function by regulating the target gene Cldn9 remained unclear.

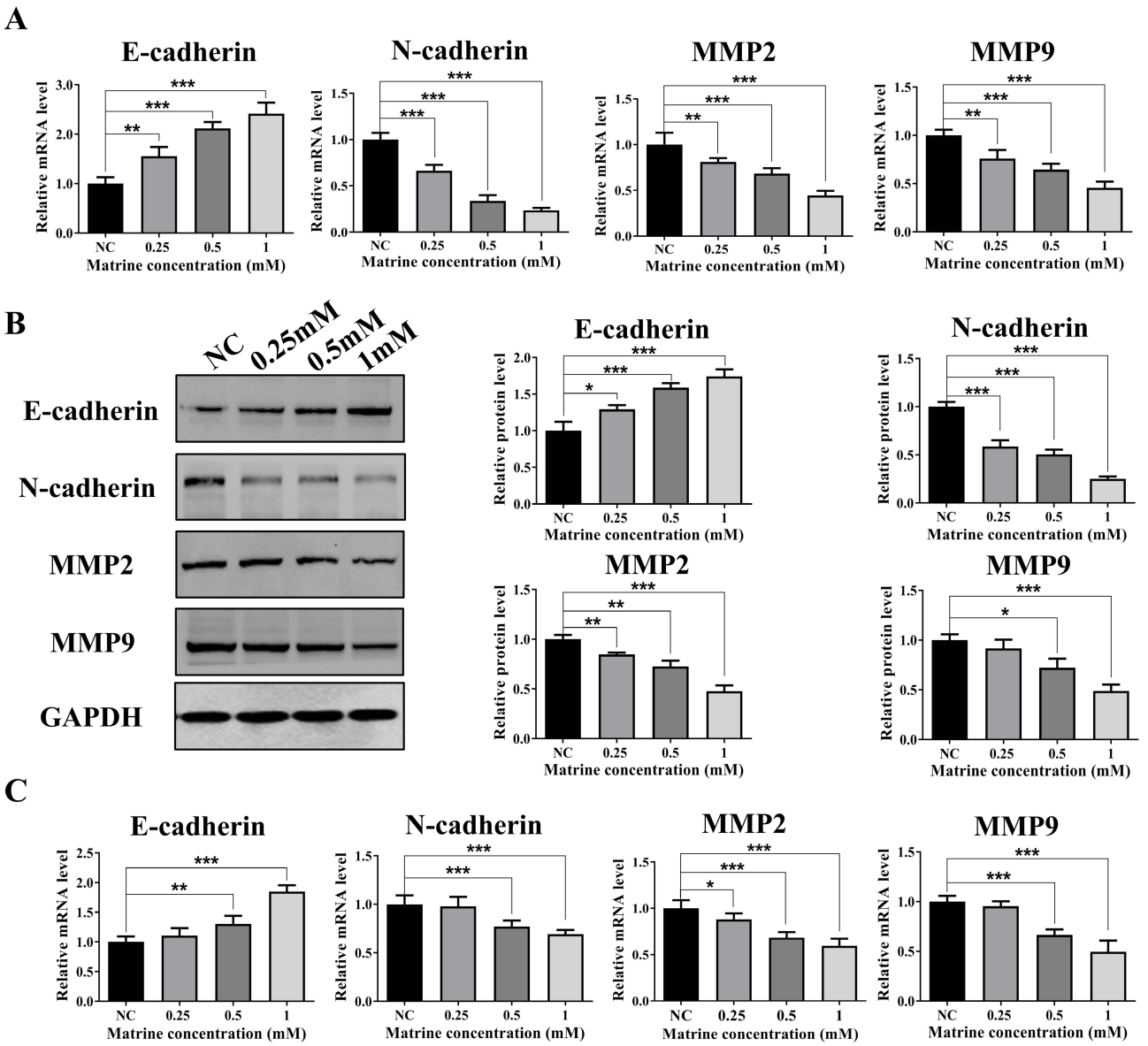

Figure 3 The effects of Mat on the key EMT factors E-cadherin, N-cadherin, MMP2, and MMP9.
Notes: (**A**) The mRNA levels of the key VM factors E-cadherin, N-cadherin, MMP2, and MMP9 in Mat treated CT26 cells; (**B**) The protein levels of the key VM factors in Mat treated CT26 cells; (**C**) The mRNA levels of the key VM factors in Mat treated SW480 cells. *p<0.05; **p<0.01; ***p<0.001.

Mat Inhibited VM Formation, Proliferation, Invasion, and Actin Filament Integrity in CT26 Cells Through Downregulation of Cldn9

To clarify whether Mat may exert inhibitory effects on CC cells by regulating the target gene Cldn9, the expression of Cldn9 was silenced by siRNA transfection and simultaneously treated with Mat. Firstly, we detected the inhibitory efficiency of Cldn9 siRNA and found that si-Cldn9-1 had a more significant downregulation of Cldn9 (Figure 6A), so it was selected for subsequent use. We then examined whether Cldn9 was associated with VM formation, and the results showed that the control group cells formed a typical VM tubular structure, while transfected with Cldn9 siRNA for 48 h obviously inhibited VM formation in CT26 cells; but when treating CT26 cells with 0.5mM Mat while silencing Cldn9 expression, the VM structure was more significantly disrupted (Figure 6B). Next, we investigated the effects of Cldn9 on proliferation, apoptosis, invasion, migration, and actin

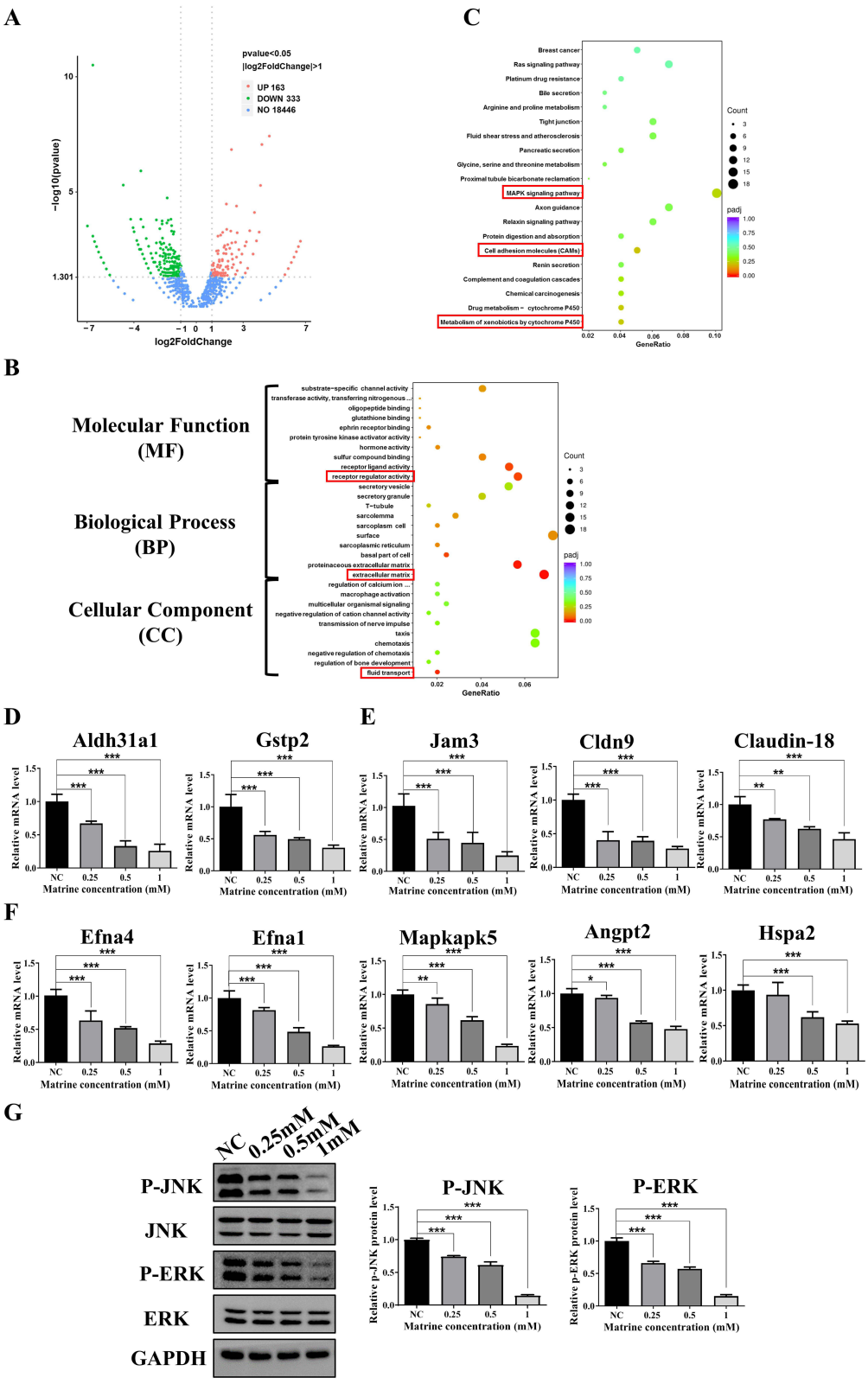

Figure 4 The differentially expressed genes (DEGs) in Mat treated CT26 cells and GO and KEGG pathway analysis.

Notes: (**A**) Volcanic map of DEGs after Mat treatment in CC CT26 cells; (**B**) KEGG pathway analysis of DEGs after Mat treatment in CT26 cells. The red boxes represent the most significantly enriched items; (**C**) GO analysis of DEGs after Mat treatment in CT26 cells. The red boxes represent the most significantly enriched items; (**D**) The mRNA expression of Aldh3a1 and Gstp2 enriched in the metabolism of xenobiotics by the cytochrome P450 were verified by qRT-PCR in Mat treated CT26 cells; (**E**) The mRNA expression of Jam3, Cldn9, and Claudin-18 enriched in cell adhesion molecules pathway were verified by qRT-PCR; (**F**) The mRNA expression of Efna4, Efna1, Mapkapk5, Angpt2, and Hspa2 enriched in the MAPK signaling pathway were verified by qRT-PCR; (**G**) The protein and phosphorylation levels of JNK and ERK in MAPK pathway detected by Western blotting. *p<0.05; **p<0.01; ***p<0.001.

https://doi.org/10.2147/DDDT.S417077 DovePress

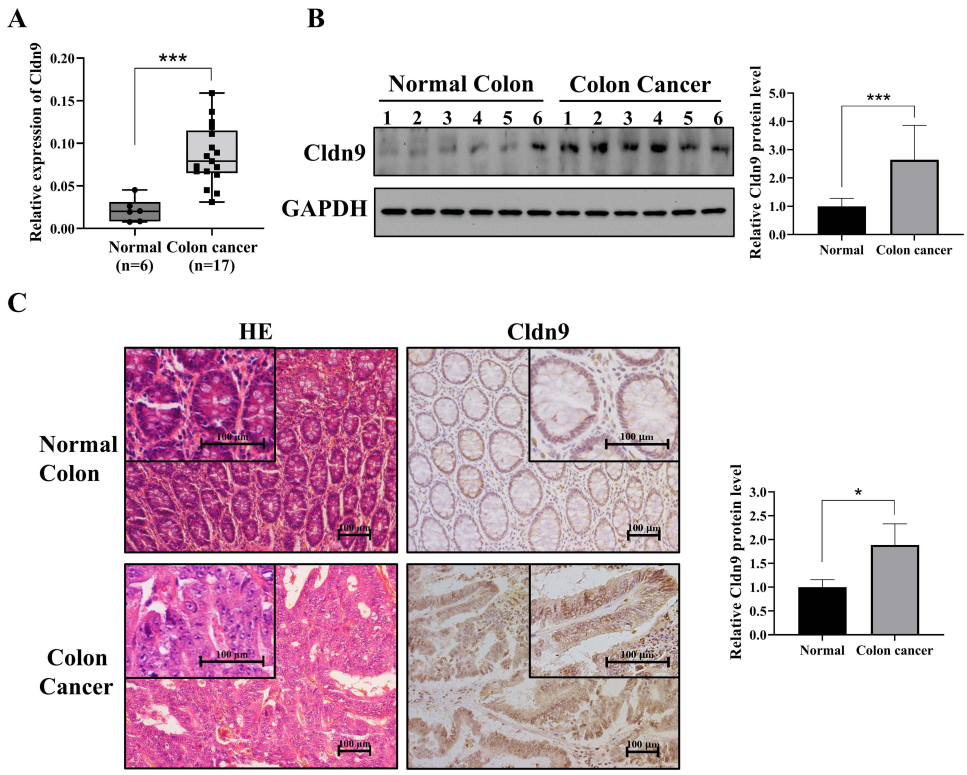

Figure 5 The expression of target gene Cldn9 in CC tissues.
Notes: (**A**) The expression of Cldn9 in human normal colon tissues and CC tissues detected by qRT-PCR; (**B**) The expression of Cldn9 in human normal colon tissues and CC tissues detected Western blotting; (**C**) The expression of Cldn9 in human normal colon tissue and CC tissue detected by immunohistochemistry. Scale bars represent 100 μm. *p<0.05; ***p<0.001.

filament integrity in CC cells. The results showed that compared with the control group, after 48 h of transfection with Cldn9 siRNA, the viability of CT26 cells significantly decreased (Figure 6C), while cell apoptosis was obviously induced (Figure 6D), cell migration and invasion were significantly inhibited (Figure 6E–G), and the morphology of intercellular microfilaments became looser and the number decreased (Figure 6H). Meanwhile, the synergistic treatment with 0.5mM Mat intensified the inhibitory effects on cell proliferation, migration, invasion, and actin filament integrity, further exacerbating the proportion of cell apoptosis (Figure 6C–H). These results indicated that Cldn9 is involved in regulating CT26 cells VM formation, proliferation, invasion, and actin filament integrity, and confirmed that the effect of Mat is consistent with the effect of down-regulating Cldn9. In addition, Mat downregulated the expression of Cldn9 and further promoted the inhibitory effect of Cldn9 knockdown on CC cells, suggesting at least that Mat may exert its pharmacological function in inhibiting CC through, but not dependent on, Cldn-9.

Mat Inhibited the EMT Process and MAPK Signaling Pathway Through Cldn9

To further clarify the mechanism of Mat-mediated inhibition of CC through Cldn9 regulation, we detected expression changes in key EMT proteins and the MAPK signaling pathway. The results showed that after Cldn9 silencing, the mRNA and protein expression levels of N-cadherin, MMP2, and MMP9 in CT26 cells were significantly downregulated compared to the control group. In addition, the expression level of E-cadherin was significantly upregulated, and the phosphorylation levels of JNK and ERK were downregulated; combined treatment with 0.5mM Mat further enhanced the above expression trends (Figure 7A–C). These results indicate that Mat may regulate the EMT-dependent and MAPK signaling pathways through Cldn9, thereby inhibiting VM formation and the proliferation, migration, and invasion of CC cells.

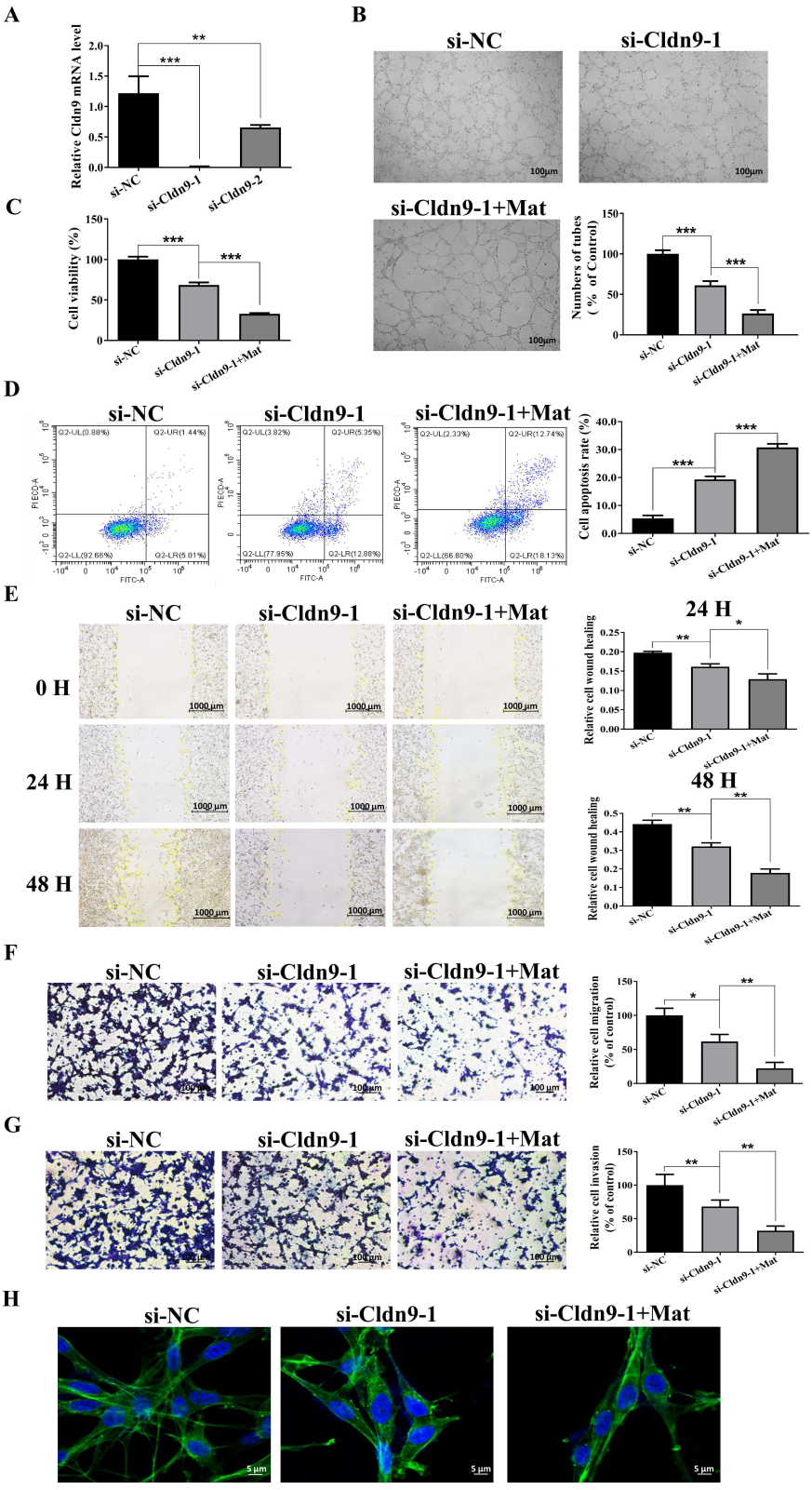

Figure 6 Effects of Cldn9 silencing and simultaneous treatment with Mat on VM formation, proliferation, invasion, and actin filament integrity in CT26 cells.
Notes: (**A**) Detection of siRNA inhibition efficiency of Cldn9; (**B**) Effects of Cldn9 silencing and simultaneous treatment with Mat on VM formation in CT26 cells. Scale bars represent 100 μm; (**C**) Effects of Cldn9 silencing and simultaneous treatment with Mat on cell viability of CT26 cells; (**D**) Effects of Cldn9 silencing and simultaneous treatment with Mat on apoptosis of CT26 cells; (**E**) Effects of Cldn9 silencing and simultaneous treatment with Mat on the migration of CT26 cells by scratch healing assay. Scale bars represent 1000 μm; (**F**) Effects of Cldn9 silencing and simultaneous treatment with Mat on the migration of CT26 cells by Transwell assay. Scale bars represent 100 μm; (**G**) Effects of Cldn9 silencing and simultaneous treatment with Mat on the invasion of CT26 cells by Transwell assay. Scale bars represent 100 μm; (**H**) Effects of Cldn9 silencing and simultaneous treatment with Mat on the integrity of actin filament in CT26 cells. Scale bars represent 5 μm. *p<0.05; **p<0.01; ***p<0.001.

https://doi.org/10.2147/DDDT.S417077 DovePress

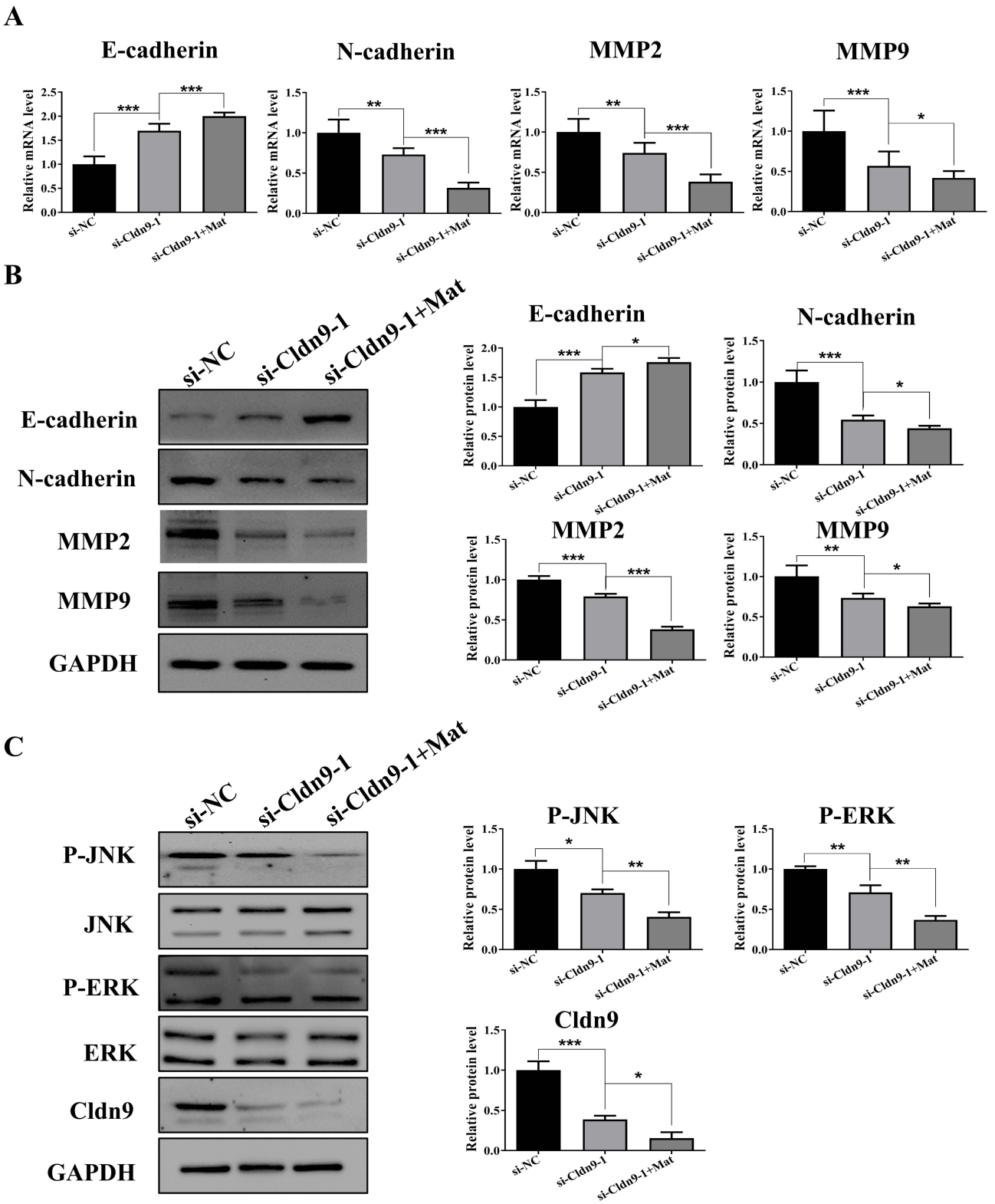

Figure 7 Effects of Cldn9 silencing and simultaneous treatment with Mat on the EMT process and MAPK signaling pathway.

Notes: (**A**) Effects of Cldn9 silencing and simultaneous treatment with Mat on mRNA levels of E-cadherin, N-cadherin, MMP2, and MMP9 in CT26 cells; (**B**) Effects of Cldn9 silencing and simultaneous treatment with Mat on protein levels of E-cadherin, N-cadherin, MMP2, and MMP9 in CT26 cells; (**C**) Effects of Cldn9 silencing and simultaneous treatment with Mat on protein levels of JNK, ERK, and Cldn9 and phosphorylation levels of JNK and ERK in CT26 cells. *p<0.05; **p<0.01; ***p<0.001.

Discussion

CC is one of the most common malignant cancers in human beings. With the aging of the population and improvements in diet and living conditions, the incidence of CC in China has increased significantly. According to the latest data from the National Cancer Center, approximately 4.57 million new cancer cases were reported in China in 2020, and the overall incidence rate of CRC jumped to second, with approximately 550,000 new cases each year. Approximately three million Chinese people died of cancer in 2020; CRC was the fifth most common cause of cancer deaths, accounting for approximately 280,000 deaths that year.[26] The main reason for this is that most people in China have only a slight awareness of colonoscopy. Most CRC patients are in the middle and late stages when diagnosed, with distant metastasis in the liver, lungs, and other organs leading to poor treatment effects.

Multiple preliminary studies have shown that VM exists in CRC and is associated with metastasis and prognosis.[12,13] Different from angiogenesis, VM has high plasticity and does not require the involvement of endothelial cells. Highly invasive tumor cells can form vascular structures on their own, promoting tumor metastasis and progression, which may be a key factor for poor tumor prognosis.[23] In this study, we demonstrated that CC cells form typical VM through 3D culture in vitro. However, the function and mechanism of Mat on VM in CC had not been reported. Our study showed that Mat inhibited VM formation in CT26 CC cells in a time- and dose-dependent manner. Mat also significantly inhibited cell proliferation, migration, and invasion, and promoted apoptosis in CT26 cells. The cytoskeleton consists of a series of filamentous structures including intermediate filaments, actin filaments, and microtubules.[27] Studies have shown that actin kinetics is usually associated with the dysregulation of cell motility and invasion.[25] In this study, we found that actin filaments were gradually destroyed and actin filament integrity was inhibited with increasing Mat concentrations, which illustrated the ability of Mat to inhibit the migration and invasion of CC cells.

Epithelial-mesenchymal transformation (EMT) is one mechanism that leads to VM. In the process of EMT, epithelial cells gradually dedifferentiate and lose cell polarity. This is manifested by decreased expression of epithelial markers (such as E-cadherin) and increased expression of interstitial markers (such as N-cadherin), leading to changes in cell morphology and behavior.[28] Cytogenetic VM undergoes a process like EMT. We detected changes in the expression of key proteins in CC cells during the EMT process following Mat treatment. The results showed that N-cadherin, MMP2, and MMP9 were significantly downregulated, while E-cadherin was significantly upregulated, suggesting that Mat may inhibit VM formation through an EMT-dependent process. Studies have shown that the expression of matrix metalloproteinases (MMPs) is closely related to the inflammatory degree that promotes the invasion and migration of tumor cells. Among these, MMP2 and MMP9 play the most important roles in tumor invasion, metastasis, and angiogenesis.[29] Here, our findings indicated that Mat inhibited the invasion and migration of cells by reducing MMPs, which also explained the scratch and transwell experiment results. This suggests that Mat blocked the motor ability of CT26 cells as a potential mechanism of VM inhibition. In addition, we also detected changes in mRNA expression of key VM factors in SW480 human CC cells after Mat treatment. The results were consistent with the trends seen in CT26 cells. Mat had a clear inhibitory effect on VM formation in CC cells, suggesting that Mat may be a promising anti-invasion and metastasis drug for CC.

To further explore the action mechanism of Mat, transcriptome sequencing was used. Results showed that 163 genes were significantly upregulated and 333 genes were significantly downregulated in CT26 CC cells after Mat intervention. GO analysis results showed that the DEGs were remarkably enriched in the fluid transport, extracellular matrix, and receptor regulator activity items. KEGG pathway enrichment analysis showed that these DEGs were significantly enriched in the metabolism of xenobiotics by cytochrome P450, cell adhesion molecules, and MAPK signaling pathways, suggesting that Mat may exert pharmacological activity mainly through the regulation of these pathways. Previous studies have shown that VM in tumors is related to HIF-1α,[30–33] VEGF,[34–38] PI3K-AKT,[39,40] MAPK,[41–43] and other signaling pathways. The imbalance between EphA2 and VEGFA activated the intracellular PI3K-AKT and MAPK signaling pathways, thereby regulating the basic functions of cells.[39–41] This may be one of the main mechanisms promoting VM formation. In this study, we found that the phosphorylation levels of key MAPK signaling pathway genes were downregulated after Mat treatment, suggesting that Mat may inhibit VM formation, cell growth, invasion, and migration of CT26 cells by inhibiting the MAPK signaling pathway. This has been partially confirmed via in vitro experiments, but the specific molecular mechanism requires further study.

An interesting finding from our RNA-sequencing results combined with the bioinformatics analysis was that many DEGs were enriched in the cell adhesion molecules signaling pathway. As membrane receptors mediating cell–cell and cell–matrix interactions, cell adhesion molecules play a crucial role in cell signal transduction and are associated with adhesion, migration, invasion, angiogenesis, and organ-specific metastasis.[44] Among them, Cldn9 attracted our attention because it is significantly downregulated after Mat treatment. Cldn9 belongs to the Claudins family, a multi-gene family first described by Shorichiro Tsukita et al. Together, the Claudins constitute an important part of the tight connections between cells and control the flow of intercellular molecules by establishing cellular barriers. Their functional changes are closely related to the occurrence of cancer in corresponding tissues.[45,46] Sharma et al[47] knocked down the expression of Cldn9 in 3LL lung cancer cells using siRNA and found that in vitro movement and invasion and in vivo metastasis of 3LL cells were inhibited. In addition, overexpression of Cldn9 enhanced the movement of cells, which proved that Cldn9 plays a significant role in promoting the metastasis of lung cancer. In addition, studies have found that[48] Cldn9 is highly expressed in pituitary oncocytoma compared with normal pituitary cells, showing the same trend in invasive oncocytoma and non-invasive oncocytoma. Therefore, Cldn9 may be a potential biomarker for invasive pituitary oncocytoma. However, no studies have explored the association between Cldn9 and the development of CC. Therefore, we hypothesized that Cldn9 may be a target of Mat and participate in its ability to inhibit VM formation, cell proliferation, invasion, and migration in CC. In this study, we firstly found that Cldn9 was upregulated in human CC tissues compared with normal tissues, and silencing Cldn9 in CT26 CC cells significantly inhibited VM formation, cell proliferation, migration, and invasion, and significantly downregulated the expression of N-cadherin, MMP2, and MMP9, as well as the phosphorylation levels of ERK and JNK, while upregulating the expression of E-cadherin. It suggests that Cldn9 may participate in the EMT process and regulate the MAPK signaling pathway to exert pharmacological effects. These findings indicated that the inhibitory effects of Mat and downregulation of Cldn9 on CC cells are consistent, and Mat further promoted the effect of Cldn9 knockdown, at least indicating that the effect of Mat may be partially achieved by downregulation of Cldn9. In addition, as is well known, the vast majority of drugs are multi-target, and in the case of knocking down Cldn9, Mat may still exert similar anti-tumor effects through the regulation of another protein, while Cldn9 is only one of its many regulated proteins. Therefore, Mat may inhibit CC cells by downregulating Cldn9 rather than relying on Cldn9 to block the EMT process and inhibit the MAPK signaling pathway.

In summary, we found for the first time that Mat affected the VM formation and actin filament integrity in CC cells, clarifying that inhibiting Cldn9 can reverse the EMT process, inhibit the MAPK signaling pathway, and thereby reduced the proliferation and invasiveness of CC cells. These findings provide a potential candidate drug and therapeutic target for VM-based anti-metastasis therapy for CC.

Acknowledgments

We thank LetPub for its linguistic assistance during the preparation of this manuscript.

Funding

This work was supported by the Natural Science Foundation of Jiangsu Province (BK20200936), the Natural Science Research Project of the Higher Educational Institutions of Jiangsu Province (20KJB320007), the Science and Technology Planning Project of Yangzhou City (YZ2021082), and the Entrepreneurship and Innovation Program of Jiangsu Province (2020-30200).

Disclosure

The authors declare no competing interests.

References

1. Sung H, Ferlay J, Siegel RL, et al. Global cancer statistics 2020: GLOBOCAN estimates of incidence and mortality worldwide for 36 cancers in 185 countries. *CA Cancer J Clin*. 2021;71(3):209–249. doi:10.3322/caac.21660
2. Wen J, Min X, Shen M, et al. ACLY facilitates colon cancer cell metastasis by CTNNB1. *J Exp Clin Cancer Res*. 2019;38(1):401. doi:10.1186/s13046-019-1391-9
3. Ronnekleiv-Kelly SM, Kennedy GD. Management of stage IV rectal cancer: palliative options. *World J Gastroenterol*. 2011;17(7):835–847. doi:10.3748/wjg.v17.i7.835

4. Luo ZF, Zhao D, Li XQ, et al. Clinical significance of HOTAIR expression in colon cancer. *World J Gastroenterol*. 2016;22(22):5254–5259. doi:10.3748/wjg.v22.i22.5254
5. Huang J, Xu H. Matrine: bioactivities and structural modifications. *Curr Top Med Chem*. 2016;16(28):3365–3378. doi:10.2174/1568026616666160506131012
6. Zhang H, Chen L, Sun X, Yang Q, Wan L, Guo C. Matrine: a promising natural product with various pharmacological activities. *Front Pharmacol*. 2020;11:588. doi:10.3389/fphar.2020.00588
7. Chen L, Chen L, Wan L, et al. Matrine improves skeletal muscle atrophy by inhibiting E3 ubiquitin ligases and activating the Akt/mTOR/FoxO3alpha signaling pathway in C2C12 myotubes and mice. *Oncol Rep*. 2019;42(2):479–494. doi:10.3892/or.2019.7205
8. Zhang X, Hou G, Liu A, et al. Matrine inhibits the development and progression of ovarian cancer by repressing cancer associated phosphorylation signaling pathways. *Cell Death Dis*. 2019;10(10):770. doi:10.1038/s41419-019-2013-3
9. Lin Y, He F, Wu L, Xu Y, Du Q. Matrine exerts pharmacological effects through multiple signaling pathways: a comprehensive review. *Drug Des Devel Ther*. 2022;16:533–569. doi:10.2147/DDDT.S349678
10. Thijssen VL, Paulis YW, Nowak-Sliwinska P, et al. Targeting PDGF-mediated recruitment of pericytes blocks vascular mimicry and tumor growth. *J Pathol*. 2018;246(4):447–458. doi:10.1002/path.5152
11. Bittner M, Meltzer P, Chen Y, et al. Molecular classification of cutaneous malignant melanoma by gene expression profiling. *Nature*. 2000;406(6795):536–540. doi:10.1038/35020115
12. Baeten CI, Hillen F, Pauwels P, de Bruine AP, Baeten CG. Prognostic role of vasculogenic mimicry in colorectal cancer. *Dis Colon Rectum*. 2009;52(12):2028–2035. doi:10.1007/DCR.0b013e3181beb4ff
13. Song X, An Y, Chen D, et al. Microbial metabolite deoxycholic acid promotes vasculogenic mimicry formation in intestinal carcinogenesis. *Cancer Sci*. 2022;113(2):459–477. doi:10.1111/cas.15208
14. Hou F, Li W, Shi Q, et al. Yi Ai Fang, a traditional Chinese herbal formula, impacts the vasculogenic mimicry formation of human colorectal cancer through HIF-1alpha and epithelial mesenchymal transition. *BMC Complement Altern Med*. 2016;16(1):428. doi:10.1186/s12906-016-1419-z
15. Zeng D, Zhou P, Jiang R, et al. Evodiamine inhibits vasculogenic mimicry in HCT116 cells by suppressing hypoxia-inducible factor 1-alpha-mediated angiogenesis. *Anticancer Drugs*. 2021;32(3):314–322. doi:10.1097/CAD.0000000000001030
16. Han C, Sun B, Zhao X, et al. Phosphorylation of STAT3 promotes vasculogenic mimicry by inducing epithelial-to-mesenchymal transition in colorectal cancer. *Technol Cancer Res Treat*. 2017;16(6):1209–1219. doi:10.1177/1533034617742312
17. Zhang S, Cheng B, Li H, et al. Matrine inhibits proliferation and induces apoptosis of human colon cancer LoVo cells by inactivating Akt pathway. *Mol Biol Rep*. 2014;41(4):2101–2108. doi:10.1007/s11033-014-3059-z
18. Liu J, Guo Y, Cao J. Matrine triggers colon cancer cell apoptosis and G0/G1 cell cycle arrest via mediation of microRNA-22. *Phytother Res*. 2020;34(7):1619–1628. doi:10.1002/ptr.6626
19. Ren H, Zhang S, Ma H, et al. Matrine reduces the proliferation and invasion of colorectal cancer cells via reducing the activity of p38 signaling pathway. *Acta Biochim Biophys Sin*. 2014;46(12):1049–1055. doi:10.1093/abbs/gmu101
20. Du Q, Hu B, Feng Y, et al. circOMA1-Mediated miR-145-5p suppresses tumor growth of nonfunctioning pituitary adenomas by targeting TPT1. *J Clin Endocrinol Metab*. 2019;104(6):2419–2434. doi:10.1210/jc.2018-01851
21. Zhou J, Wang T, Dou Y, et al. Brusatol ameliorates 2, 4, 6-trinitrobenzenesulfonic acid-induced experimental colitis in rats: involvement of NF-kappaB pathway and NLRP3 inflammasome. *Int Immunopharmacol*. 2018;64:264–274. doi:10.1016/j.intimp.2018.09.008
22. Shi J, Han G, Wang J, et al. Matrine promotes hepatic oval cells differentiation into hepatocytes and alleviates liver injury by suppression of Notch signalling pathway. *Life Sci*. 2020;261:118354. doi:10.1016/j.lfs.2020.118354
23. Sun B, Zhang D, Zhao N, Zhao X. Epithelial-to-endothelial transition and cancer stem cells: two cornerstones of vasculogenic mimicry in malignant tumors. *Oncotarget*. 2017;8(18):30502–30510. doi:10.18632/oncotarget.8461
24. Liu Q, Qiao L, Liang N, et al. The relationship between vasculogenic mimicry and epithelial-mesenchymal transitions. *J Cell Mol Med*. 2016;20(9):1761–1769. doi:10.1111/jcmm.12851
25. Okegawa T, Pong RC, Li Y, Hsieh JT. The role of cell adhesion molecule in cancer progression and its application in cancer therapy. *Acta Biochim Pol*. 2004;51(2):445–457. doi:10.18388/abp.2004_3583
26. Rongshou Zheng SZHZ, Zhang S, Zeng H. Cancer incidence and mortality in China, 2016. *J Natl Cancer*. 2022;2(1):1–9. doi:10.1016/j.jncc.2022.02.002
27. Chazotte B. Labeling cytoskeletal F-actin with rhodamine phalloidin or fluorescein phalloidin for imaging. *Cold Spring Harb Protoc*. 2010;2010(5):t4947. doi:10.1101/pdb.prot4947
28. Dongre A, Weinberg RA. New insights into the mechanisms of epithelial-mesenchymal transition and implications for cancer. *Nat Rev Mol Cell Biol*. 2019;20(2):69–84. doi:10.1038/s41580-018-0080-4
29. Guo W, Gao X, Zhan R, Zhao Z, Xu K, Tang B. Tricolor imaging of MMPs to investigate the promoting roles of inflammation on invasion and migration of tumor cells. *Talanta*. 2021;222:121525. doi:10.1016/j.talanta.2020.121525
30. Zhang JG, Zhou HM, Zhang X, et al. Hypoxic induction of vasculogenic mimicry in hepatocellular carcinoma: role of HIF-1 alpha, RhoA/ROCK and Rac1/PAK signaling. *BMC Cancer*. 2020;20(1):32. doi:10.1186/s12885-019-6501-8
31. Du J, Sun B, Zhao X, et al. Hypoxia promotes vasculogenic mimicry formation by inducing epithelial-mesenchymal transition in ovarian carcinoma. *Gynecol Oncol*. 2014;133(3):575–583. doi:10.1016/j.ygyno.2014.02.034
32. Wang M, Zhao X, Zhu D, et al. HIF-1alpha promoted vasculogenic mimicry formation in hepatocellular carcinoma through LOXL2 up-regulation in hypoxic tumor microenvironment. *J Exp Clin Cancer Res*. 2017;36(1):60. doi:10.1186/s13046-017-0533-1
33. Tang NN, Zhu H, Zhang HJ, et al. HIF-1alpha induces VE-cadherin expression and modulates vasculogenic mimicry in esophageal carcinoma cells. *World J Gastroenterol*. 2014;20(47):17894–17904. doi:10.3748/wjg.v20.i47.17894
34. Xu S, Bai J, Zhuan Z, et al. EBV-LMP1 is involved in vasculogenic mimicry formation via VEGFA/VEGFR1 signaling in nasopharyngeal carcinoma. *Oncol Rep*. 2018;40(1):377–384. doi:10.3892/or.2018.6414
35. Schnegg CI, Yang MH, Ghosh SK, Hsu MY. Induction of vasculogenic mimicry overrides VEGF-A silencing and enriches stem-like cancer cells in melanoma. *Cancer Res*. 2015;75(8):1682–1690. doi:10.1158/0008-5472.CAN-14-1855
36. Wang JQ, Gao YS, Mei J, Xue HM, Wang SQ, Cai XS. [Morphological changes in osteosarcoma xenografts in nude mice after inhibiting angiogenesis by Ad-VEGF-siRNA]. *Ai Zheng*. 2009;28(6):581–586. Chinese.

37. Takahashi H, Shibuya M. The vascular endothelial growth factor (VEGF)/VEGF receptor system and its role under physiological and pathological conditions. *Clin Sci*. 2005;109(3):227–241. doi:10.1042/CS20040370
38. Xu X, Zong Y, Gao Y, et al. VEGF induce vasculogenic mimicry of choroidal melanoma through the PI3k signal pathway. *Biomed Res Int*. 2019;2019:3909102. doi:10.1155/2019/3909102
39. Ding X, Xi W, Ji J, et al. HGF derived from cancer-associated fibroblasts promotes vascularization in gastric cancer via PI3K/AKT and ERK1/2 signaling. *Oncol Rep*. 2018;40(2):1185–1195. doi:10.3892/or.2018.6500
40. Lu XS, Sun W, Ge CY, Zhang WZ, Fan YZ. Contribution of the PI3K/MMPs/Ln-5gamma2 and EphA2/FAK/Paxillin signaling pathways to tumor growth and vasculogenic mimicry of gallbladder carcinomas. *Int J Oncol*. 2013;42(6):2103–2115. doi:10.3892/ijo.2013.1897
41. Ling G, Ji Q, Ye W, Ma D, Wang Y. Epithelial-mesenchymal transition regulated by p38/MAPK signaling pathways participates in vasculogenic mimicry formation in SHG44 cells transfected with TGF-beta cDNA loaded lentivirus in vitro and in vivo. *Int J Oncol*. 2016;49(6):2387–2398. doi:10.3892/ijo.2016.3724
42. Wang F, Chen F, Hu W, Zhang Y. Mig-7 gene silencing inhibits vasculogenic mimicry formation and invasion of glioma U251 cells in vitro by suppressing MEK/ERK signaling. *Nan Fang Yi Ke Da Xue Xue Bao*. 2019;39(5):566–571. doi:10.12122/j.issn.1673-4254.2019.05.11
43. Huang B, Xiao E, Huang M. MEK/ERK pathway is positively involved in hypoxia-induced vasculogenic mimicry formation in hepatocellular carcinoma which is regulated negatively by protein kinase A. *Med Oncol*. 2015;32(1):408. doi:10.1007/s12032-014-0408-7
44. Li DM, Feng YM. Signaling mechanism of cell adhesion molecules in breast cancer metastasis: potential therapeutic targets. *Breast Cancer Res Treat* 2011, 128(1): 7–21. doi:10.1007/s10549-011-1499-x
45. Singh P, Toom S, Huang Y. Anti-claudin 18.2 antibody as new targeted therapy for advanced gastric cancer. *J Hematol Oncol* 2017, 10(1): 105. doi:10.1186/s13045-017-0473-4
46. Li W, Zong S, Shi Q, Li H, Xu J, Hou F. Hypoxia-induced vasculogenic mimicry formation in human colorectal cancer cells: involvement of HIF-1a, Claudin-4, and E-cadherin and Vimentin. *Sci Rep*. 2016;6:37534. doi:10.1038/srep37534
47. Sharma RK, Chheda ZS, Das PB, Gomez-Gutierrez JG, Jala VR, Haribabu B. A spontaneous metastasis model reveals the significance of claudin-9 overexpression in lung cancer metastasis. *Clin Exp Metastasis* 2016, 33(3): 263–275. doi:10.1007/s10585-015-9776-4
48. Hong L, Wu Y, Feng J, Yu S, Li C, Wu Y, Li Z, Cao L, Wang F, Zhang Y. Overexpression of the cell adhesion molecule claudin-9 is associated with invasion in pituitary oncocytomas. *Hum Pathol* 2014, 45(12): 2423–2429. doi:10.1016/j.humpath.2014.08.006